

# The role of crystalline defects and the density of a graphite foil in the laser-induced degradation

Sergei I. Kudryashov,\* Sergei N. Borisov, Sergei G. Ionov and Nikita B. Zorov

Department of Chemistry, M. V. Lomonosov Moscow State University, 119899 Moscow, Russian Federation. Fax: +7 095 932 8846; e-mail: [serg@laser.chem.msu.su](mailto:serg@laser.chem.msu.su)

The differences in the efficiency of laser-induced degradation of foil samples of thermally expanded graphite are determined by differences in the density of the foil and in the concentration of nonequilibrium crystallite defects in the starting thermally expanded graphite and depend on the thermodynamics of carbon evaporation in the vicinity of the critical point.

Under conditions of laser vaporisation, low-density carbon materials are promising sources of large carbon clusters.<sup>1,2</sup> However, the thermodynamics and mechanisms of laser-induced vaporisation of these materials have scarcely been studied until now. For systematic studies of the behaviour of low-density carbon materials under the action of laser radiation, it is of interest to use the graphite foil (GF) obtained from thermally expanded graphite (TEG), because its physicochemical properties (density, microstructure, texture and concentration of nonequilibrium chemically and thermally induced crystallite defects) can be varied. We have studied the physicochemical properties of graphite foil in recent years.<sup>3,4</sup> We found that GF is a low-density carbon material consisting of separate weakly bound crystallites (with a thickness of about 0.01  $\mu\text{m}$ ) oriented nearly parallel to the foil surface and possessing, at a density of 0.5–0.7  $\text{g cm}^{-3}$ , 70–80% porosity (according to the low-angle X-ray scattering data, the average pore size is 10–20 nm). Because of the high porosity of the structure, the GF absorbance  $A(629 \text{ nm}) = 0.9$  in the near-surface region (up to 100 nm in thickness at a density of 0.7  $\text{g cm}^{-3}$ ) approaches this parameter for the ideal black body, and the velocities of propagation of acoustic and thermal waves in the material dramatically decrease.<sup>3</sup> In the region of radiation absorption, quasi-equilibrium evaporation into the pores of the foil (the average pore diameter is shorter than the free path length of vapour particles) occurs, and depending on the ratio between the material density  $\rho$  and the density of carbon in the critical state ( $\rho_{\text{cr}} = 0.64 \text{ g cm}^{-3}$ ),<sup>5</sup> the subcritical ( $\rho \leq \rho_{\text{cr}}$ ), critical, and supercritical ( $\rho > \rho_{\text{cr}}$ )<sup>6</sup> states of the substance can occur in the pores. Due to the presence of nonequilibrium defects, the GF structure is metastable; therefore, the heats of laser-induced phase transitions in GF can differ from similar characteristics for crystalline graphite.

In this work, the effects of the bulk density of GF and the concentration of nonequilibrium defects on the thermodynamics of laser evaporation of GF were studied by the optoacoustic procedure of measuring the average depth of the crater  $X$  per laser pulse.<sup>7</sup> Graphite foil was vaporised in air by focused

radiation of the second harmonic of an Nd:YAG laser [wavelength 532 nm, pulse energy 5 mJ, pulse width (FWHM) 25 ns, and pulse repetition rate 12.5 Hz] in the laser power density range  $I_0$  0.01–3  $\text{GW cm}^{-2}$ . The GF samples with densities of 0.5  $\text{g cm}^{-3}$  (nos. 1–3,  $\rho < \rho_{\text{cr}}$ ) and 0.7  $\text{g cm}^{-3}$  (nos. 4 and 5,  $\rho > \rho_{\text{cr}}$ ) obtained by rolling (without binders) of TEG that was prepared by thermal treatment of hydrolysed intercalated graphite compounds with sulfuric acid at 1200–1300 K<sup>8</sup> were examined. The GF samples with different concentrations of nonequilibrium defects were obtained by variations in the conditions of the synthesis of graphite bisulfate and the temperature of the thermal treatment. The previously studied<sup>9</sup> sample of polycrystalline graphite (PCG, 1.7  $\text{g cm}^{-3}$ ) was chosen as reference sample no. 6.

Since the mechanism of substance removal under the action of pulsed laser radiation on GF samples was not known beforehand, we considered the overall process as sample degradation taking into account the entire set of related processes (heating, melting, evaporation, vapour absorption, etc.). The specific depth of a crater  $X/(rI_0)$  [Figure 1(a)], which takes into account the difference in the densities of different graphite samples ( $r$  is the ratio of the sample density to the density of crystalline graphite 2.2  $\text{g cm}^{-3}$ ), was considered as the efficiency of the degradation at different  $I_0$  values. Using laser time-of-flight mass spectroscopy, we obtained other characteristics of the degradation of graphite materials, viz., temperatures of the substance in the region of the hot core and in the expansion zone of the laser plume. These values were determined by Saha's equation from the ratio of intensities of multiply charged atomic carbon ions (up to triply charged) and from the expression for the half-width of the Maxwell distribution of velocities for the laser plume particles, respectively.

The experimental dependences of  $X/(rI_0)$  on  $I_0$  [Figure 1(a)] show that there are two characteristic ranges of  $I_0$  in which the behaviour of the graphite materials is fundamentally different. At  $I_0 > 1 \text{ GW cm}^{-2}$ , the degradation proceeds similarly for all of the graphite materials: the efficiency of degradation  $X/(rI_0)$

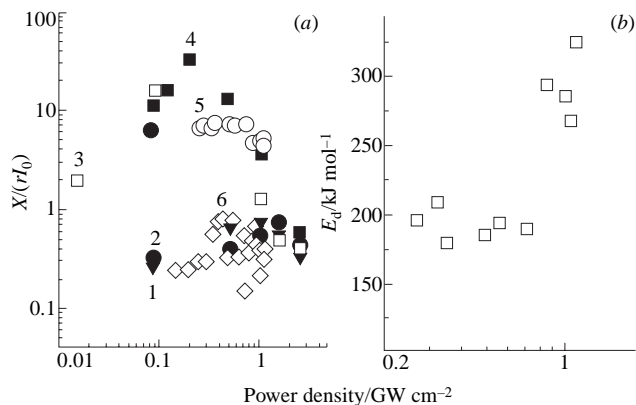


**Figure 1** (a) Dependences of the specific depth of a crater  $X/(rI_0)$  [ $\mu\text{m}(\text{GW cm}^{-2})^{-1}$ ] on the laser power density for different graphite samples (GF sample numbers are indicated); (b) dependence of the degradation energy per mole of the substance on  $I_0$  for GF sample no. 5.

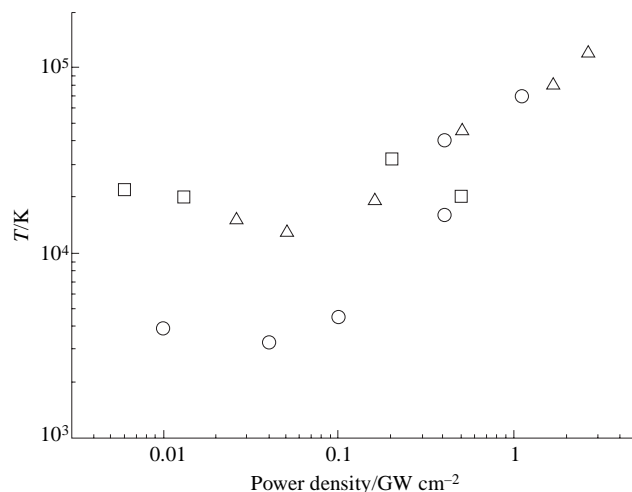


**Figure 2** Maximum temperature of laser plume particles as a function of  $I_0$  for GF sample nos. 5 ( $\square$ ) and 1 ( $\triangle$ ) and a PCG sample ( $\circ$ ).

decreases gradually. Judging from the increase in the maximum plume temperature in the hot core and expansion zone (Figure 2), this is due to substantial absorption of radiation by the degradation products and screening of the target. By contrast, in the region of moderate values  $I_0 < 1 \text{ GW cm}^{-2}$ , differences in the properties of the test materials appear [Figures 1(a) and 2]. These materials can be subdivided into two groups by the efficiency of decomposition  $X/(rI_0)$ .

The group with higher efficiency of decomposition contains the GF sample nos. 4, 5 ( $0.7 \text{ g cm}^{-3}$ ) and 3 ( $0.5 \text{ g cm}^{-3}$ ) with high defect concentrations. The second group with low efficiency consists of the low-defect GF sample nos. 1 and 2 with a bulk density of  $0.5 \text{ g cm}^{-3}$  as well as PCG sample. The comparison of the GF sample nos. 1–3 with the same density and different defect concentrations shows that it is the latter factor that plays the determining role in the laser-induced degradation of these materials.

It has been shown in ref. 6 that the degradation of the low-density high-defect GF sample no. 5 proceeds *via* hydrodynamic removal of the substance (carbon in the supercritical state) from the laser-heated surface layer of the target. A similar process of hydrodynamic removal of a vapour–liquid mixture of the products of spinodal decomposition of the labile liquid carbon phase takes place in the surface vaporisation of the PCG sample.<sup>9</sup> Therefore, differences in the efficiency of degradation likely appear during the formation of the final (before degradation) state of carbon rather than at the stage of removal (due to plasma formation and screening of the target surface). In order to study the energetics of degradation of the GF samples, we calculated the deposited energy per mole of removed substance (degradation energy  $E_d$ ) resulting from the absorption of laser radiation in the target:

$$E_d = \frac{AV_m}{X} \int I(t) dt \quad (1)$$

where  $V_m$  and  $A$  are the molar volume and the absorbance of the samples, respectively. When the GF absorbance is about 0.9, the degradation energies  $E_d$  are approximately  $50 \text{ kJ mol}^{-1}$  for GF sample nos. 3 and 4 in the  $I_0$  range  $0.1\text{--}1 \text{ GW cm}^{-2}$  and  $193 \pm 8 \text{ kJ mol}^{-1}$  for sample no. 5 [Figure 1(b),  $0.2\text{--}0.7 \text{ GW cm}^{-2}$ ]. For the PCG sample and GF sample nos. 1 and 2, the degradation energy is as high as  $500 \text{ kJ mol}^{-1}$  in the  $I_0$  range  $0.1\text{--}0.3 \text{ GW cm}^{-2}$ , and it is approximately halved at  $I_0 > 0.3 \text{ GW cm}^{-2}$ .

Thus, it can be noted that the heat of formation of the supercritical state of carbon ( $\geq 270 \text{ kJ mol}^{-1}$ )<sup>10</sup> that is formed by laser vaporisation of high-defect GF sample nos. 4 and 5 ( $\rho > \rho_{cr}$ ) decreases to the degradation energies of these samples resulting from the contribution of the energy of nonequilibrium defects of crystallites (about 220 and  $80 \text{ kJ mol}^{-1}$ , respectively). The degradation energies of low-density GF sample nos. 1 and 2 ( $\rho < \rho_{cr}$ ) and the PCG sample correspond to the enthalpy of formation of carbon vapour with subcritical parameters (*ca.*  $500 \text{ kJ mol}^{-1}$ )<sup>10,11</sup> in the laser power density range  $0.1\text{--}0.3 \text{ GW cm}^{-2}$  and to the enthalpy of formation of the liquid

carbon phase in the labile state ( $\geq 270 \text{ kJ mol}^{-1}$ )<sup>10</sup> at  $I_0 > 0.3 \text{ GW cm}^{-2}$ . An anomalously low (about  $50 \text{ kJ mol}^{-1}$ ) value of the degradation energy for the low-density high-defect GF sample no. 3 ( $\rho < \rho_{cr}$ ) in the  $I_0$  range  $0.1\text{--}0.5 \text{ GW cm}^{-2}$  is explained by fast transition of the liquid carbon phase to the labile state almost without consumption of energy for evaporation ( $265 \text{ kJ mol}^{-1}$ ),<sup>11</sup> which is favoured by a decrease in the heat of formation of the labile state (*ca.*  $270 \text{ kJ mol}^{-1}$ )<sup>10</sup> by the energy of nonequilibrium defects (*ca.*  $220 \text{ kJ mol}^{-1}$ ).

This work was supported by the Russian Foundation for Basic Research (grant no. 98-03-32679).

## References

- 1 H. Y. So and C. L. Wilkins, *J. Phys. Chem.*, 1989, **93**, 1184.
- 2 I. J. Dance, K. J. Fisher and G. D. Willet, *J. Phys. Chem.*, 1991, **95**, 8425.
- 3 S. I. Kudryashov, S. V. Sokolov, N. B. Zorov, A. A. Karabutov and Yu. Ya. Kuzyakov, *Mendeleev Commun.*, 1997, 25.
- 4 L. A. Monyakina, V. V. Avdeev, I. V. Nikol'skaya and S. G. Ionov, *Zh. Fiz. Khim.*, 1995, **69**, 926 (*Russ. J. Phys. Chem.*, 1995, **69**, 842).
- 5 H. R. Leider, O. H. Krikorian and D. A. Young, *Carbon*, 1973, **11**, 555.
- 6 S. I. Kudryashov, S. G. Ionov, A. A. Karabutov and N. B. Zorov, *Mendeleev Commun.*, 1998, 212.
- 7 S. I. Kudryashov, A. A. Karabutov, N. B. Zorov and Yu. Ya. Kuzyakov, *Mendeleev Commun.*, 1996, 96.
- 8 V. A. Kulbachinskii, S. G. Ionov, S. A. Lapin and A. G. Mandrea, *Phys. Chem. Solids*, 1996, **57**, 893.
- 9 S. I. Kudryashov, A. A. Karabutov and N. B. Zorov, *Mendeleev Commun.*, 1998, 6.
- 10 *Termodinamicheskie svoistva individual'nykh veshchestv (Thermodynamic Properties of Individual Substances)*, ed. V. P. Glushko, Nauka, Moscow, 1979, vol. 2, p. 10 (in Russian).
- 11 A. V. Kirillin, M. D. Kovalenko and M. A. Sheindlin, *Teplofizika Vysokikh Temperatur*, 1985, **23**, 699 (in Russian).

Received: Moscow, 8th June 1998

Cambridge, 10th August 1998; Com. 8/04736G